# Reliable Optimized Structures with High Performance Continuous fiber thermoplastic composites from Additive manufacturing (AM)

Danning Zhang, Natalie Rudolph, Peter Woytowitz

AREVO Inc
Milpitas, CA/USA

## ABSTRACT

Additive Manufacturing (AM) is still one of the fastest growing manufacturing areas. While metal AM parts are more and more used for structural applications, few plastic AM parts and processes provide sufficient durability for this purpose. One of the problems is related to the lack of reliable material data for design as well as missing component level tests. Therefore, simulation efforts are progressing at slow speeds and often cannot be validated with experimental data. AREVO has overcome this challenge with its Direct Energy Deposition (DED) process that is capable to process carbon fiber volume contents of 50% and more as well as its modeling and software capabilities.
In this paper, the mechanical properties including tension, compression, flexural, interlaminar shear, open hole tension and compression, fracture toughness, impact resistance and compression strength after impact (CAI) of the AREVO materials are reported. It can be seen that the mechanical properties are comparable with traditionally manufactured continuous carbon fiber thermoplastic composites. Using this data, the performance of structural components is simulated through an integrated approach considering the processing condition and tool path. The example of a simple structural element is presented here. Good agreement was achieved from the simulation and experimental testing, highlighting the reliability of the AREVO process and software capabilities.

## 1. INTRODUCTION

### 1.1 Additive Manufacturing in general

Additive Manufacturing (AM) encompasses a wide variety of different technologies, which have been grouped into seven major categories by the American Society for Testing and Materials (ASTM) group "ASTM F42 Additive Manufacturing". Within each category the differences between technologies are very big and every month new variations emerge. In addition, the anisotropy of almost all AM parts, make the required testing programs much larger than for other processes that yield more isotropic material properties. Therefore, efforts to standardize tests and obtain high fidelity data sets are progressing slowly and are very expensive.

At the same time, measuring this data for faster and improved product design is only viable for processes that are suitable to produce end-use parts. Thus, larger efforts so far have mostly focused on the metal and polymer powder bed fusion processes, e.g. in the Additive Manufacturing Benchmark Test Series (AM-Bench) by NIST [1]. In addition, many research



*SAMPE Conference Proceedings. Charlotte, NC, May 20-23, 2019. Society for the Advancement of Material and Process Engineering – North America.*

groups have worked on understanding the Material Extrusion (ME) process due to the low cost of those 3D printers and the required material. However, most data is not comparable, shows wide variation and is not suitable for more than a few end-use applications due to reduced part performance compared to conventional, high volume manufacturing technologies [2-11].

One way to improve the performance of material extruded parts is the incorporation of fibers. While short fibers can increase the stiffness of the parts, continuous fibers can also increase the strength and toughness by several orders of magnitude. As there are no significant changes to the equipment required to print with short fibers, this has been done for several years now on different scales from desktop 3D printers to Big Area Additive Manufacturing (BAAM) machines. The use of continuous fiber reinforcement has much bigger benefits, but requires modifications to the print head or new processes altogether. There are three different variations of the Material Extrusion process with continuous carbon fibers (CCF): 1) where a preimpregnated filament is fed into the nozzle, 2) where a dry fiber roving is impregnated inside of the nozzle and 3) a combination of the two where a preimpregnated feedstock is embedded into more plastic material inside the nozzle.

All of these processes have in common that the adhesion at the layer interface is achieved by heat conduction from the extruded material to the previous deposited layer. A review of the resulting performance of these different processes was published by Brenken et al. [12] and shows their low yield compared to the theoretical strength of these materials as well as the wide variation of strength and modulus with very similar systems. An alternative that results in better interfacial adhesion and significantly higher fiber volume content will be presented in the following.

### 1.2 The AREVO Direct Energy Deposition (DED) Process

The schematic of the AREVO DED process is shown in Figure 1. A filament is rapidly heated through a laser source. Then a compaction roller provides sufficient pressure to compress the filament and bond it to the substrate layers, eliminating the voids inside and in between the layers, and consolidating the parts in-situ. The entire deposition system is mounted on a six axis robot, allowing the deposition in any angle and direction. The deposition is controlled in a close loop and can be tailored to any given material and geometric feature.

The consolidation quality and the mechanical performance of the material produced by the AREVO DED process will be presented in this paper. Besides the high quality materials, the software is capable to provide reliable design for engineering parts, which is another significant aspect that drives the technology to manufacture structural applications. A full study of mechanical properties of AREVO composites was conducted, which provided valuable input and validation for the simulation, and enabled the reliable structure design and optimization with the software.

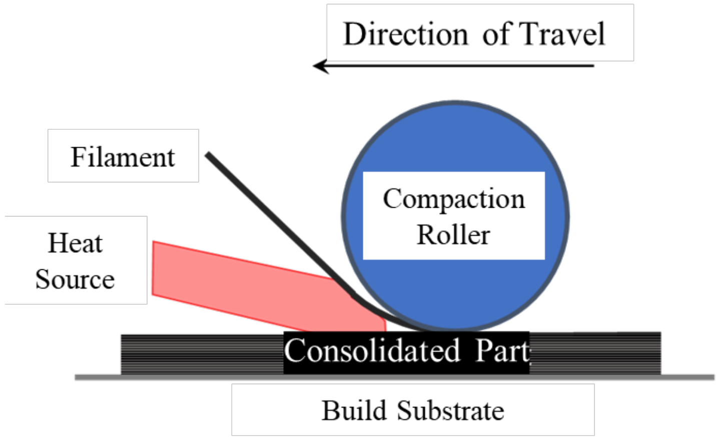


*Figure 1. Schematic of AREVO DED process*

## 2. EXPERIMENTATION

### 2.1 Sample Printing and Preparation

The filament used consists of continuous standard aerospace grade carbon fibers (CF) and poly ether ether ketone (PEEK) thermoplastic resin. The nominal fiber volume fraction is 50%, and the void content present in the filament is smaller than 2%. A typical micrograph of the filament cross section is shown in Figure 2. Panels with unidirectional and quasi-isotropic (QI, [-45º/90º/45º/0º]ns) fiber layup directions were fabricated with the DED process. After the panels were printed, coupons with different dimensions were cut for microscopy analysis and mechanical testing.

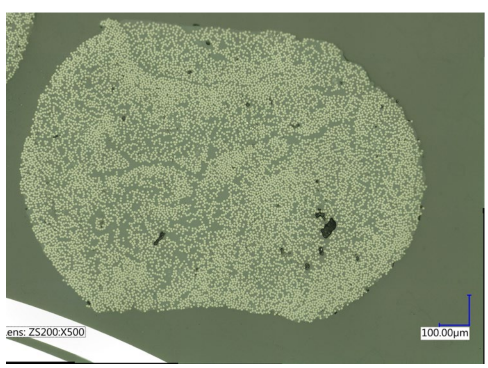


*Figure 2. A typical micrograph of the cross section of the filament used in the AREVO DED process.*

## 2.2 Microscopy

Samples from representative regions of the printed panels were polished with a Buehler Ecomet 250 polishing wheel, with SiC grinding paper and polishing particles down to 0.01 μm. The cross-sectional micrographs of the samples were obtained with a Keyence VHX6000 microscope under 300X magnification. With the stitching function of the microscope and its software, the entire cross section of each sample can be captured. Then, the images were analyzed in Image J. The void pixels were picked up by setting the threshold on the intensity histogram of the entire composites region of the image. The void content was the ratio of the number of pixels for the void region and the total number of pixels of the composite region. The void content of each printed part was obtained by averaging more than 5 images.

## 2.3 Mechanical Testing

### *2.3.1 Tensile, Compressive, and Flexural Tests*

Since AREVO materials contain continuous carbon fibers with high fiber content and show the characteristic anisotropic behavior, the mechanical tests follow ASTM standards for fiber reinforced polymer matrix composite materials. ASTM D3039, ASTM D6641, ASTM D7264 are adopted for tensile, compression and flexural tests, respectively. The tests were conducted with an Instron 3369 with maximum load capacity of 50 kN. The coupon dimensions and test details are listed in Table 1. At least 5 coupons were tested for each test configuration.

*Table 1 Coupon dimensions and details for tensile, compressive, and flexural tests*

| Test | Lay-up | Thickness (mm) | Width (mm) | Length (mm) | Test Speed (mm/min) |
|---|---|---|---|---|---|
| Tensile | 0° | 1.5 | 15 | 250 | 2 |
| | [-45°/90°/45°/0°]s | 4 | 25 | 250 | 2 |
| Compression | 0° | 2 | 30 | 140 | 1.3 |
| | [-45°/90°/45°/0°]s | 4 | 30 | 140 | 1.3 |
| Flexural | 0° | 4 | 13 | 154 | 1 |
| | [-45°/90°/45°/0°]s | 4 | 13 | 154 | 1 |

### *2.3.2 Interlaminar Shear Tests*

The interlaminar property was examined through the short beam shear test, following ASTM D2344. Unidirectional coupons were tested. The setup is shown in Figure 3. The coupon geometry was set to 36 mm long by 12 mm wide and 6 mm thick so as to promote the desired interlaminar failure mode. Specimens were loaded in a three-point bend fixture with a span length of 24 mm at 1.0 mm/min. At least 5 samples were tested. The yield load ($P_y$) was recorded along with the specimen width ($b$) and thickness ($h$) so that the short beam strength ($F^{sbs}$) could be calculated per equation (1):

$$F^{sbs} = 0.75 \times \frac{P_y}{b \times h} \quad (1)$$

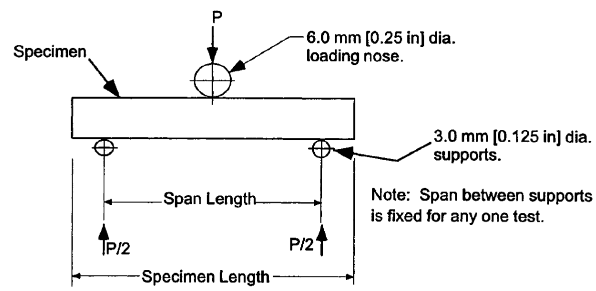


*Figure 3. Three-point bend test per ASTM D2344 [13].*

### *2.3.3 Open Hole Tension and Compression Tests*

Open hole tension and compression performance is important when designing engineering structures with composite materials. ASTM D5766 and ASTM D6484 were followed to test QI materials. The nominal thickness and width for the test coupons are 4 mm and 36 mm, respectively. The length for tension coupons is 250 mm, and 300 mm for the compression coupons. Center holes with a diameter of 6.32 mm were notched on each coupon. The test speed for both tests was 1.3 mm/min, and 5 coupons each were tested. The tension and compression strengths based on the gross width of the coupons were obtained.

### *2.3.4 Fracture Toughness $G_{Ic}$ and $G_{IIc}$*

Fracture toughness of Mode I opening $G_{Ic}$ and Mode II in-plane shear $G_{IIc}$ were obtained according to the ASTM D5528 double cantilever beam (DCB) test and the ASTM D7905 end-notched flexural (ENF) test, respectively. Unidirectional coupons with the fiber direction along the coupon length direction were used for both tests. The initial cracks were generated by inserting Kapton films of 13 μm halfway during the printing process at one end of the samples. Figure 4 (a) shows the setup of the DCB test, where coupons were bonded with loading blocks (1inch bond length). A fixture designed by the Center for Composite Materials at University of Delaware (UD-CCM) was used to apply load through the tensile fixtures. A traveling camera was placed in front of the test coupons to record the crack opening. The dimensions of the DCB coupons are 120 mm in length, 20 mm in width, 3 mm thickness, and the initial crack was 50 mm. The ENF tests were done with a three-point flexural test fixture as shown in Figure 4 (b), and the coupon dimensions are 130 mm in length, 20 mm in width, 3 mm thickness, and an initial crack of 30 mm.

*(a)* *(b)*

*Figure 4. Test set-up of the fracture toughness tests: (a) Double cantilever beam test and (b) End-notch flexural testing (photos provided by UD-CCM)*

#### *2.3.5 Impact and Compression After Impact （CAI）Tests*

To examine the impact resistance and the damage tolerance of the DED printed materials, QI coupons were tested with the ASTM D7136 falling weight impact and ASTM D7137 compression after impact tests. The coupon dimensions were 150 mm × 100 mm × 5 mm. The coupons are impacted with 5.3 kg projectile from a height of 694 mm. The impact energy was 6.67 J/mm. The coupons were Ultrasonic C-scanned with a 5 MHz probe before and after the impact test. The damaged area, dent depth and the energy absorbed were determined after the impact tests. Compression test with the fixture as specified in ASTM D7137 was used to obtain the static compressive strength after the impact tests.

## 3. RESULTS

### 3.1 Microstructure

The representative microstructures of the unidirectional and quasi-isotropic parts are shown in Figure 5. From the unidirectional sample in Figure 5 (a), it can be seen that although some fiber fold lines originally from the filament are still presented, single filaments can be hardly distinguished from the microstructure. This indicates a high level of homogeneity of the microstructure and good bonding between strips and layers. It is also noticed that the void content in the UD sample is very low, typically smaller than 1% for the unidirectional part. For the QI parts in Figure 5 (b), the individual layers show similar homogeneity as the UD part. However, interlayer voids can be sometimes contained locally in between the contact layers with off angles. This is likely due to the local variation of the dimensions and quality of the filament and can be further reduced with optimized process settings and tight dimensional control of the filament used.

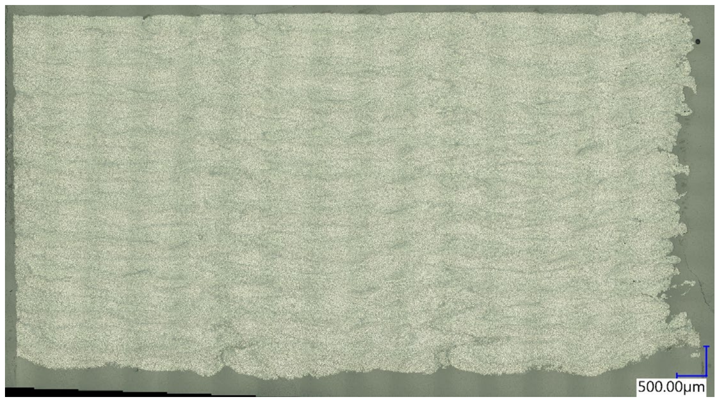


(a)

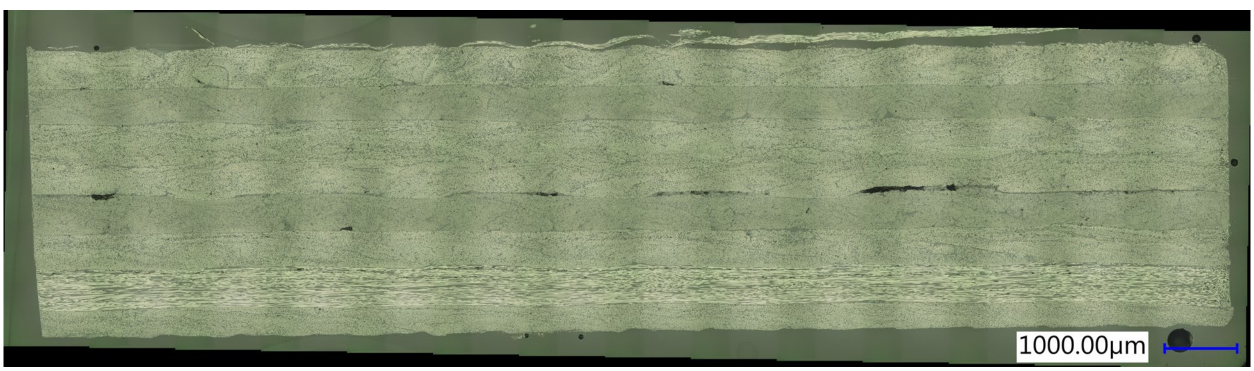


(b)

*Figure 5. Representative micrograph of (a) unidirectional (void content =0.02%) and (b) quasi-isotropic parts (void content = 0.63%) from AREVO DED process*

As an in-situ consolidation process for thermoplastic composites, this DED process is able to achieve low void content and even reduce the voids originally from the filaments. This is observed without post consolidation with an autoclave, which are often needed to reach such a low void content. [14-16] The post consolidation usually also requires vacuum bagging, molding and long cycle times, resulting in long total cycle time for a part. With the consolidation quality achieved, the AREVO DED process can eliminate the whole post consolidation process and produce parts more efficiently and effectively, especially for components with complex geometries.

Compared with other existing AM technologies, the AREVO DED process can work with filaments reinforced with continuous carbon fibers, and with much higher fiber content (>50%) [12], utilizing both the advantages of the light and strong carbon fibers, and the flexibility and sustainability of the 3D printing process.

## 3.2 Mechanical Testing

### *3.2.1 Tensile, Compressive, Flexural and Short Beam Strength*

The results of the tensile, compression and flexural tests of UD and QI coupons are summarized in Table 2. The tensile properties were compared with those of materials from other AM technologies in Figure 6 It is clearly seen that AREVO DED parts performs much better than continuous carbon fiber reinforced materials from the material extrusion (ME) technologies. The AREVO UD 0º coupons have both strength and modulus more than 2 times higher than the highest reported in the literature for the 3D printed continuous carbon fiber materials measured in fiber direction [12], and more than 14 and 22 time higher than the modulus and strength of the 3D printed chopped carbon fiber nylon 12 measured in bead direction, respectively [17]. Tensile failure strain for the UD and QI laminate are 1.22 ± 0.06 % and 1.18 ± 0.09%, respectively. Both are much higher than a typical high performance carbon fiber thermosetting composite material [18].

The tensile and compressive properties of the AREVO materials are also compared with the gold standard performance CF/PEEK parts produced in an autoclave with the same fiber content, shown in Figure 7 [19]. It is seen that the modulus of both the UD 0º and QI are comparable to those from autoclave parts, and the strength are equal or higher than 70% of the strength of autoclave parts, which is really difficult to achieve with other in-situ consolidation or out-of-autoclave (OOA) processes for thermoplastic composite materials [14,20].

*Table 2 Results from the tensile, compressive, and flexural tests*

| Test | Lay-up | Modulus (GPa) | Strength (MPa) |
|---|---|---|---|
| Tensile | 0º | 115 ± 2 | 1420 ± 83 |
| | [-45º/90º/45º/0º]s | 41 ± 3 | 479 ± 66 |
| Compressive | 0º | 100 ± 2 | 712 ± 47 |
| | [-45º/90º/45º/0º]s | 37 ± 2 | 280 ± 26 |
| Flexural | 0º | 104± 1 | 1173 ± 64 |
| | [-45º/90º/45º/0º]s | 31 ± 2 | 492 ± 54 |

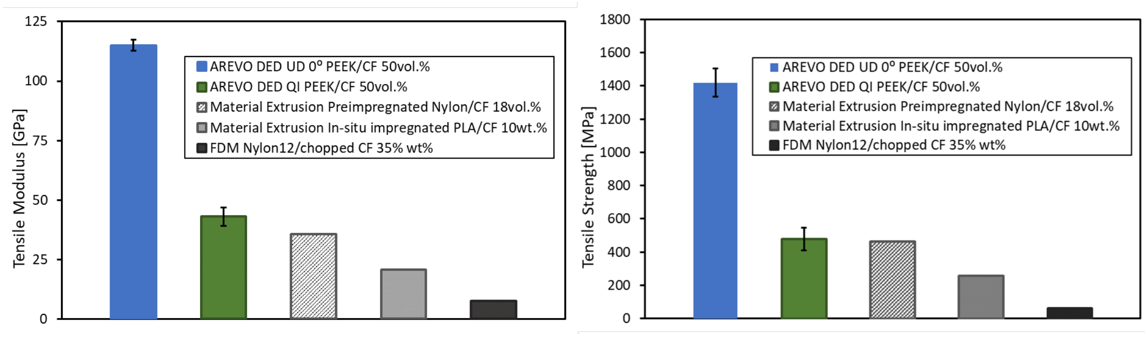


*Figure 6. Comparison of the UD tensile properties of materials from AREVO DED process and other existing AM technologies utilizing continuous or chopped carbon fibers measured in fiber and bead direction, respectively [12, 17]*

The short beam strength of AREVO UD 0º was tested as 62 ± 4 MPa, which is higher than most of the in-situ consolidation processes without post consolidation [14, 20]. The failure features interlaminar shear failure, with face compression observed under the loading point.

The high performance of the material and process allows the manufacturing of a wide range of engineering structural applications, which other additive manufacturing processes using polymeric materials can rarely do.

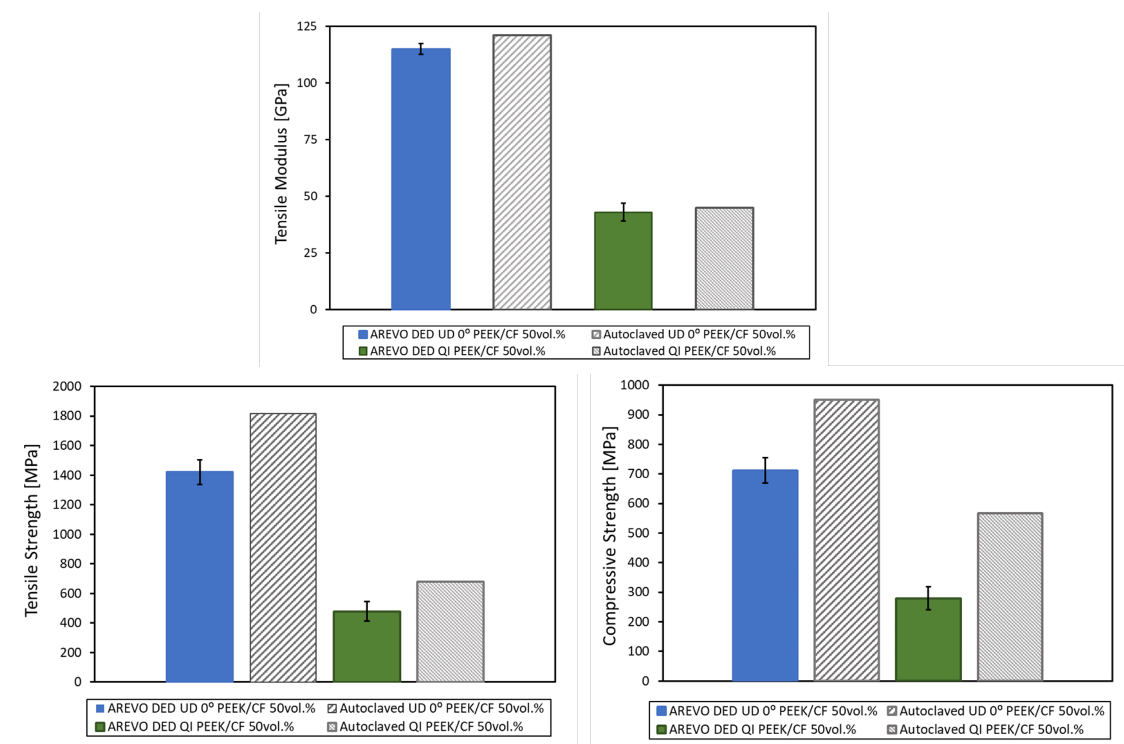


*Figure 7. Comparison of the tensile and compressive properties of carbon/PEEK composites from AREVO DED process and autoclave with fiber content of 50% [19]*

### *3.2.2 Open Hole Tension and Compression Strength*

The open hole tension and compression strength of QI coupons are 382 ± 40 MPa and 202 ± 3 MPa, respectively. Thus, the tensile strength is 23% and the compressive strength 28% lower than the ultimate tension and compression strength of the unnotched coupons. The pictures of the failed coupons are presented in Figure 8 and Figure 9, respectively. The failure in the tensile tests is mostly at the region near the holes with delamination, fiber fracture and splitting. For the compression test coupons, the failure shows lateral compressive failure in the middle gage region with fiber kinking and fracture.

*Figure 8. Failure of the Open Hole Tension coupons*

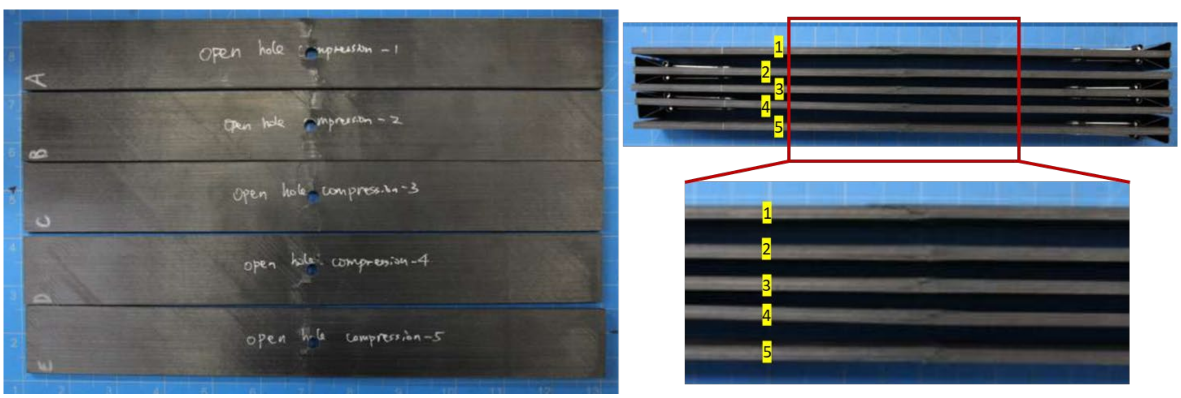


*Figure 9. Failure of the Open Hole Compression coupons*

### *3.2.3 Fracture Toughness*

The representative load vs. extension curves during the DCB and ENF tests are shown in Figure 10. The non-linear behavior during the load and unload cycle in the ENF test show the benefit of the ductile PEEK resin. The GIc and GIIc results are presented in Table 3 and compared with other composite material data from literature. It becomes clear that the fracture toughness of AREVO material is very close to the CF/PEEK composites produced with traditional processes such as autoclave, compression molding, etc. The slightly higher toughness of AREVO material could be a result of the faster cooling rates and thus lower crystallinity (32% vs. theoretical 38%) of the PEEK matrix after the AREVO in-situ consolidation process. Compared to thermosetting composite materials, the fracture toughness of AREVO CF/PEEK composite is significantly higher.

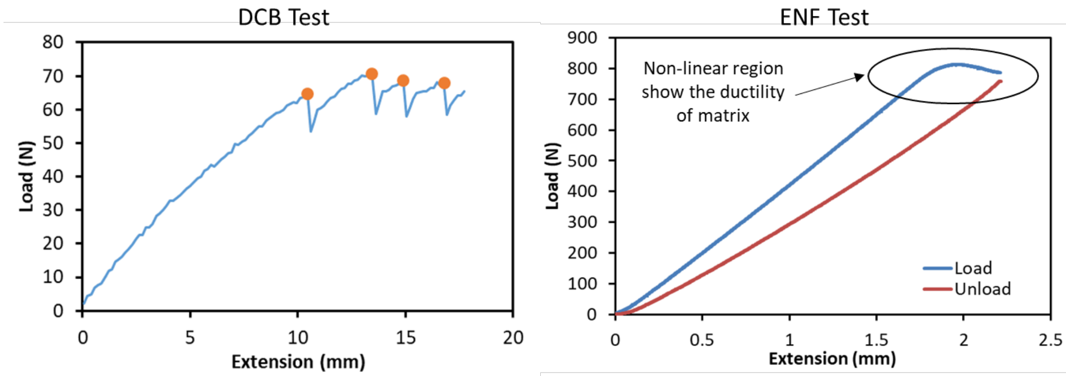


*Figure 10. Representative load vs. extension curves during the fracture toughness testing*

*Table 3 Fracture toughness of AREVO CF/PEEK 50 vol.% and other composite materials*

| Material | $G_{Ic}$ ($KJ/m^2$) | $G_{IIc}$ ($KJ/m^2$) |
|---|---|---|
| AREVO CF/PEEK 50 vol.% | 1.5 ± 0.3 | 1.4 ± 0.1 |
| AS4/PEEK 52 vol.% [20] | 1.1 – 1.4 | 1.1 |
| AS4/PEEK 61 vol.% [20] | 1.0 – 2.5 | 1.2 – 1.4 |
| CYCOM 5276-1 [21] | 0.4 | 2.4 |
| Thermosetting prepregs [22] | - | 0.6 – 1.2 |

### *3.2.4 Impact Resistance and Compression Strength after Impact*

Before and after the falling weight impact tests, the QI coupons were ultrasonic C-scanned as shown in Figure 11. It is seen that delamination occurred from the coupon center where the projectile was in contact with the coupon, and cracks propagated in all four directions to form the radial damage shape, which is typical for QI composite materials. The dent depth, damage area, the total energy absorbed and the CAI strength are listed in Table 4. The CAI strength reduced to 45% of the ultimate strength of the material without impact, which is comparable to that of hot pressed AS4/APC2 composites [23]. The failure of the coupons after the CAI tests are shown in Figure 12. Sample 1 shows an all through failure in the gage but away from the impact damage region, and sample 4 shows the compression damage through the width of the coupon in the middle region. All other three coupons have compression failure at the middle region to one lateral edge of the coupon. All the failures are commonly observed and acceptable failure modes listed in ASTM D7137. It can be clearly seen that even when impacted with the high energy of 36 J, the compressive residual strength is still higher than those from many injection molded filled and unfilled polymer materials.[24,25] Compared to 3D printed parts from neat polymer and short fiber reinforced polymer, the continuous carbon fiber reinforced composites produced in DED process is highly impact resistant and damage tolerant.

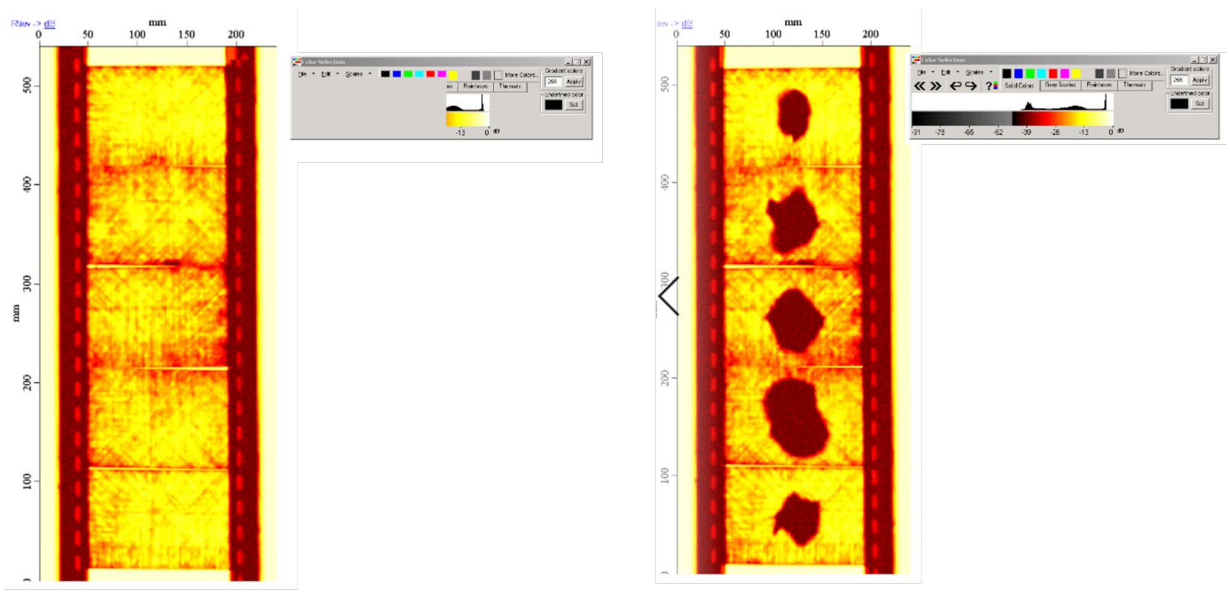

*(a)* *(b)*

Figure 11. C-scan images of the QI coupons (a) before and (b) after the impact

*Table 4 Impact and CAI test results of AREVO CF/PEEK 50 vol.% QI coupons*

| Property | Value |
|---|---|
| Depth (mm) | 0.83 ± 0.18 |
| Damage area ($mm^2$) | 2453 ± 925 |
| Energy absorbed (J) | 13.2 ± 3.1 |
| CAI strength (MPa) | 126.7 ± 17.5 |

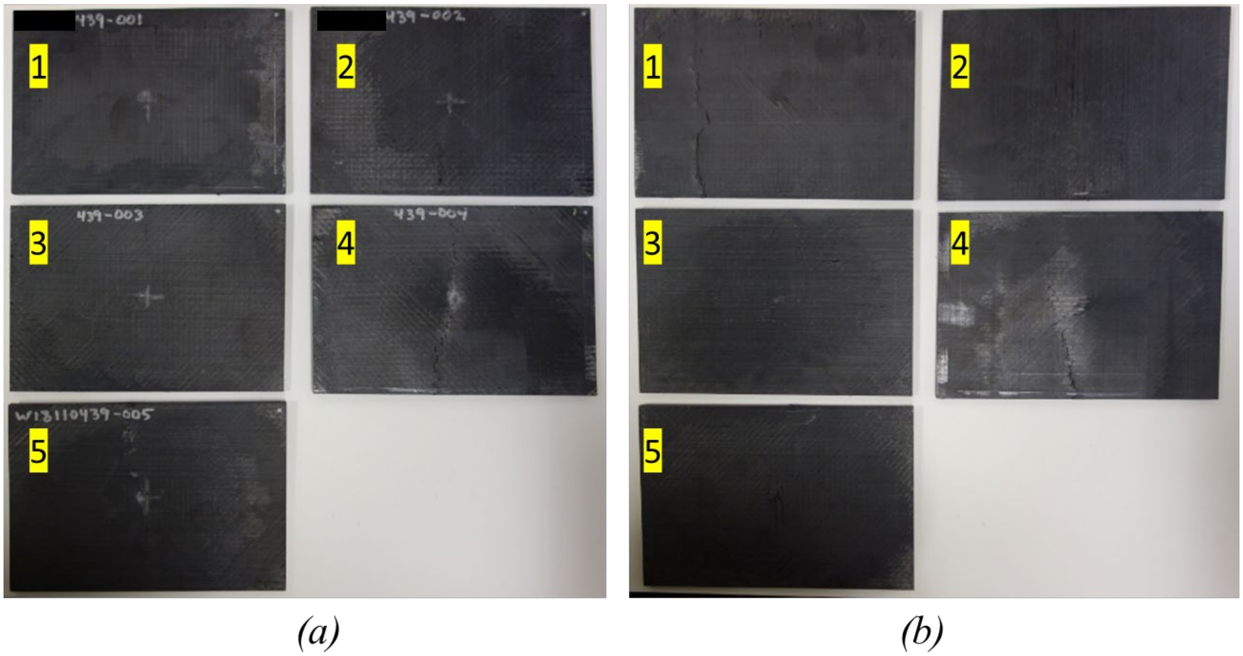


*Figure 12. Failed coupons after CAI tests (a) front and (b) back*

In summary, the presented data shows that the DED process results in parts comparable to high performance composites manufactured in an autoclave or similar high quality processes rather than other AM technologies. However, at the same time, the process enables complex features not possible in conventional composite manufacturing processes.

In the following section the applicability of traditional composite prediction tools for this DED process will be discussed.

# 4. COMPOSITES DESIGN WITH MEASURED MATERIAL PROPERTIES

## 4.1 AREVO Strength Data and Analytical Failure Criteria

Directly measuring strength data for common laminates provides the best approach for predicting the efficiency and factors of safety for strength. In cases where a high amount of tests are needed, complex stress states exist (combinations of shear and axial stress) and for cases where the stress distribution is non-uniform, measured data can be used as input to an analytical failure criteria. The analytical failure criteria typically uses limited test data, e.g. unidirectional layup. The analytical failure criteria can then be used to predict failure stresses for more complex laminates (e.g. $0^o/90^o/+45^o/-45^o$) and load cases. Here we use the unidirectional strength data along with unidirectional shear data from the DED process to predict strength of other laminates, and compare these results to actual measured data for those printed laminates.

Many analytical failure criteria have been suggested, the WWFE (world-wide failure exercise) involved many failure criteria experts and compared results against test data for a variety of materials [26]. Based on internal studies the focus was placed on the maximum stress (Max-Stress) criteria. However, we have found that using the standard Max-Stress criteria, which checks both fiber and matrix failure in a ply-by-ply fashion, was overly conservative. It was found that by modifying the maximum stress criteria to consider “fiber dominated” failure modes (where they exist) produced much better comparison to our measured failure data. In addition, several other failure criteria including “Max-Strain”, Tsai-Wu and Tsai-Hill [26] were investigated. Based on the DED data we have developed the “Maximum Stress Fiber Dominated (Max-Stress FD)” failure criteria which best predicts the performance of our materials.

The standard “Max-Stress” failure criteria is shown in Figure 13. Here, *FS* stands for “factor-of-safety” with the *t* and *c* superscripts denoting tension and compression failure, respectively. A factor of safety ≤1 indicates failure, otherwise, the analytical failure criteria predicts no failure.

$$FS^t_1 = S^t_1 / |\sigma_{11}| \quad \text{if} \quad \sigma_{11} > 0$$

$$FS^c_1 = S^c_1 / |\sigma_{11}| \quad \text{if} \quad \sigma_{11} < 0$$

$$FS^t_2 = S^t_2 / |\sigma_{22}| \quad \text{if} \quad \sigma_{22} > 0$$

$$FS^c_2 = S^c_2 / |\sigma_{22}| \quad \text{if} \quad \sigma_{22} < 0$$

$$FS^t_3 = S^t_3 / |\sigma_{33}| \quad \text{if} \quad \sigma_{33} > 0$$

$$FS^c_3 = S^c_3 / |\sigma_{33}| \quad \text{if} \quad \sigma_{33} < 0$$

$$FS_{12} = S_{12} / |\sigma_{12}| \;,\; FS_{23} = S_{23} / |\sigma_{23}| \;,\; FS_{31} = S_{31} / |\sigma_{31}|$$

where

$S^t_1$ , $S^c_1$ - Ultimate tension and compression strengths in principal material direction 1

$S^t_2$ , $S^c_2$ - Ultimate tension and compression strengths in principal material direction 2

$S^t_3$ , $S^c_3$ - Ultimate tension and compression strengths in principal material direction 3

$S_{12}$ - Ultimate shear strength associated with shear in the 1-2 plane

$S_{23}$ - Ultimate shear strength associated with shear in the 2-3 plane

$S_{31}$ - Ultimate shear strength associated with shear in the 3-1 plane

Figure 13. Standard Max-Stress Failure Criteria

The Max-Stress FD criteria differs from the traditional maximum stress criteria, in that, if a laminate has a variety of fiber directions (e.g. not unidirectional) we switch to the fiber dominated failure mode to predict failure, and, we ignore predictions of matrix failure when fibers transverse the matrix in nearby layers (or regions). Figure 14 shows comparison of standard “Max-Stress FD”, “Tsai-Hill 3D” and the “Max-Stress” with AREVO data for three lay-up configurations. The Max-Stress FD provides the best correlation, with the standard "Max-Stress" and "Tsai-Hill 3D" criteria being overly conservative for QI and [0/60º/-60º]s.

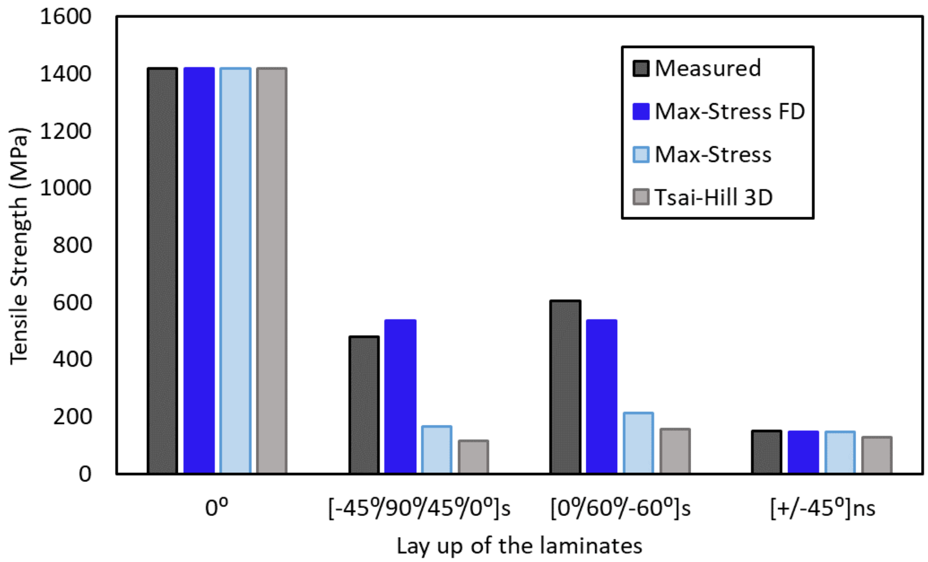


Figure 14. Comparison of AREVO measured strength and predicted results with Max Stress FD, Max-Stress, and Tsai-Hill failure criteria, showing the strength results obtained from Max Stress FD criteria agree best with the measured data

In Figure 15 the strength data of CF/PEEK material with fiber volume content of 60% measured by Jen & LEE [27] is compared with the predictions based on the Max-Stress FD and Tsai-Hill 3D criteria. It is seen that the measured results have higher strength levels compared with the 50 vol% DED materials introduced in the previous sections, which is mainly due to the higher fiber content and improved consolidation from the autoclave process. The data also shows that the Max-Stress FD failure criteria provides reasonable assessment of laminate strength similar to that obtained using Tsai-Hill 3D. Jen & Lee used the Tsai-Hill failure criteria for their study of static and fatigue strength.

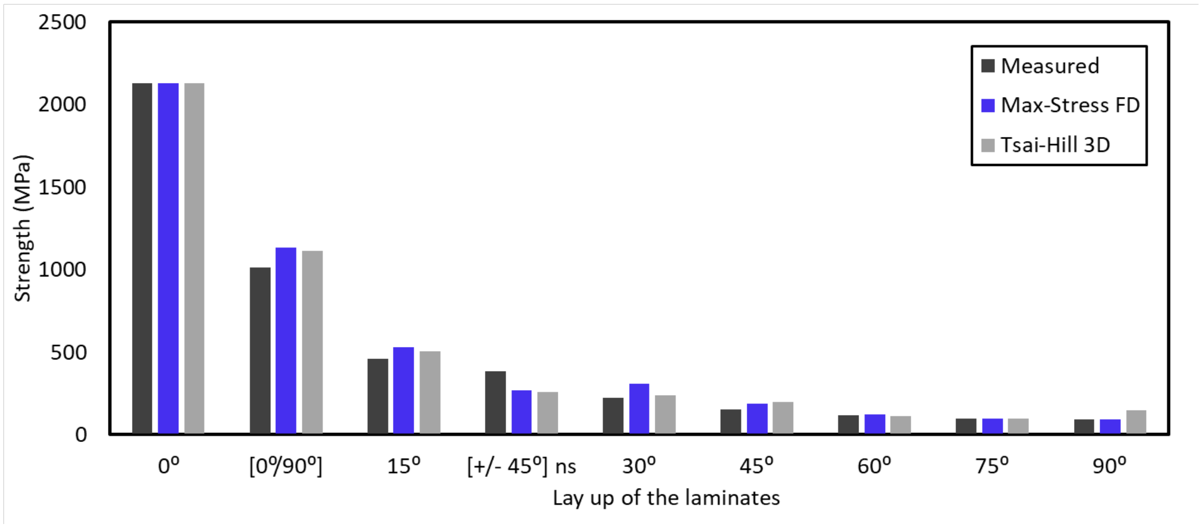


Figure 15. Comparison of strength predicted with Max-Stress FD and Tsai-Hill 3D failure criteria, and the measured results from Jen & Lee [27], showing the results from Max-Stress FD criteria correlate reasonably well to the measured results

### 4.2 Box Beam Stress Analysis and Strength Assessment

Box beams are common structural elements. Being able to customize and make small production lots or even one-offs represents a manufacturing opportunity for Additive Manufacturing. The box beam geometry shown in Figure 16 has a length of 300 mm with nominal wall thickness of 2 mm. Depending upon the use case and loading, different printing strategies should be utilized. The proposed design was analyzed using the AREVO design software Pathfinder with material properties presented in the above sections along with the previously discussed Max-Stress FD failure criteria. Displacements, stresses and failure were predicted. This analysis showed that depending upon the precise support conditions at the end, we may not realize the full strength of the design. It was predicted (based on the expected boundary conditions) that large shear stresses near the support precluded development of the full box beam strength. These shear stress concentrations which are induced due to the support conditions are shown in the lower portion of Figure 16. Based upon these predictions, the failure was predicted to occur near the support at a level of 10 kN.

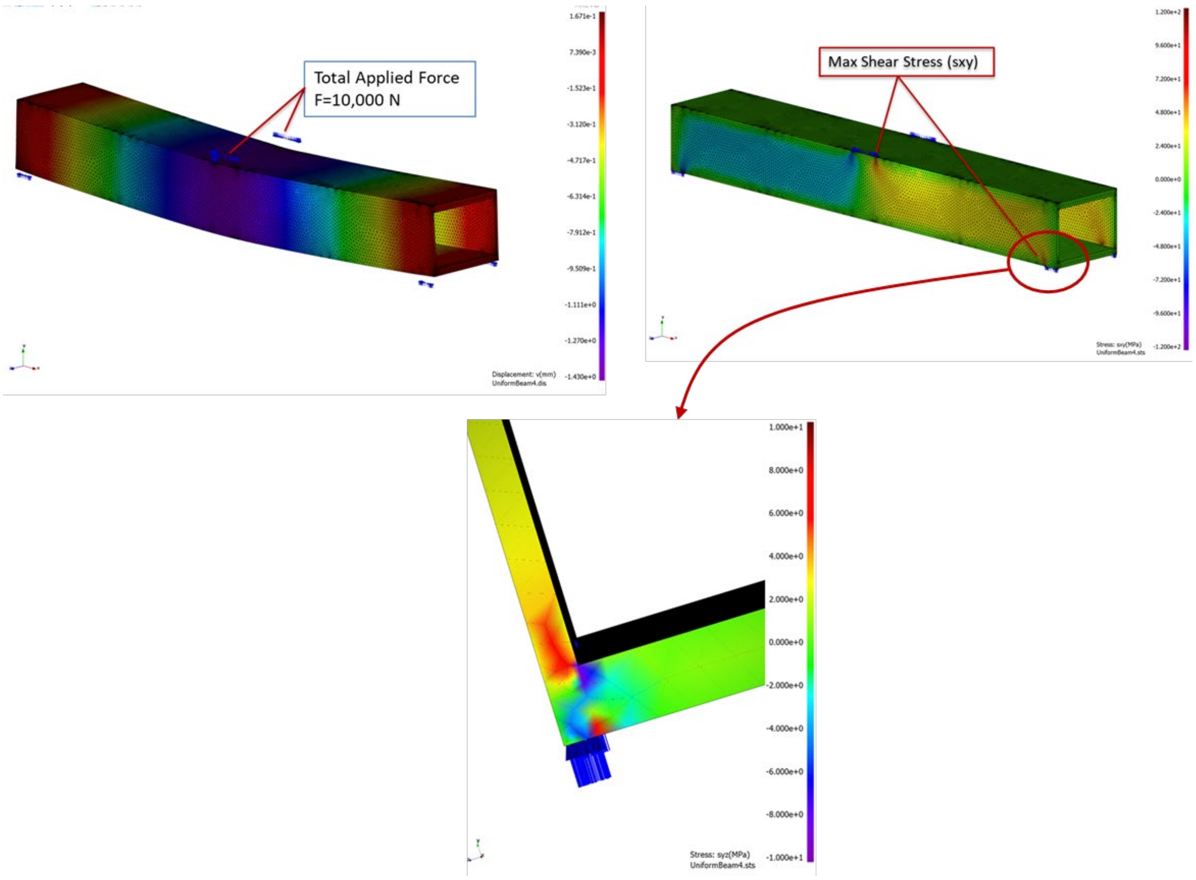


Figure 16 Finite Element Simulation of Box Beam with AREVO Pathfinder Software

Figure 17 shows the box beam previously analyzed as built (a) and under 3-point bending load (b). The average observed failure load for three samples tested was 11.4 kN. The observed failure load matches well with the predicted failure load and represents an 11% error in prediction, with the prediction being a conservative (underestimated) of the actual performance. Based on the Max-Stress FD criteria, it was found that the failure is dominated by the shear strength ($\sigma_{yz}$) in this case.

(a) (b)

Figure 17 The box beam (a) as built and (b) during testing

The applicability of traditional composite prediction tools for this DED process, enables designers to create new composite designs based on a comprehensive set of data and a structural analysis of various complex load cases experienced during the service life of a component. One of the first structural parts presented are rideable 3D printed bike frames with or without electrical drive. The case study showcasing the design and production of such a bike frame was published here [28]

## 5. CONCLUSIONS

The presented mechanical performance achieved with the AREVO DED process is in good agreement with mechanical data for similar fiber and matrix materials, fiber contents and layups found in literature. It can be seen that the performance even compares to thermoplastic composite parts manufactured in the autoclave, which is the only process that eradicates all the defects from the material and the processing, such as voids, resin rich areas, and delamination. All of these issues have a detrimental effect on the mechanical performance of the components. Therefore, autoclaved components show the highest strength and stiffness compared to parts produced with other manufacturing technologies. In comparison to autoclave and other traditional process technologies, the DED process allows in-situ consolidation of the thermoplastic composite parts with good interfacial adhesion due to direct heating at the interfaces. At the same time, the process enables complex features only possible with AM technologies. Among these features are hollow sections like the box beams, thin, curved walls as well as overhangs, which were recently showcased in a 3D printed bike frame.

In addition to the high performance and complexity of the parts produced with the DED process, the strength computed with the Max-Stress Fiber Dominated failure criteria was found to provide excellent agreement with the measured strength of various lay-up configurations from the DED process and the literature [27]. This shows that in contrast to other AM technologies, the good predictability of the anisotropy of the materials regardless of missing data sets reduces the amount of tests required start designing more complex components. What is more, it allows to create reliable designs for the service life of these end-use components. This not only accelerates the design process from month or weeks to days, but also makes it less expensive. This, in addition to minimizing the tooling cost, allowing the production of customized products, and reducing the manufacturing time of the final products, is truly shifting the paradigm of manufacturing.

## 6. ACKNOWLEDGEMENT

The authors would like to thank the Center of Composite Materials at University of Delaware for providing the facilities for parts of the mechanical testing, especially Dr. Nicholas Shevchenko for his effort on obtaining the fracture toughness, impact and CAI performance of the materials, and the consulting support from Prof. Jack Gillespie.

# 7. REFERENCES


1. N.N., Additive Manufacturing Benchmark Test Series, https://www.nist.gov/ambench, accessed on Jan 29, 2019.
2. S.-H. Ahn, M. Montero, D. Odell, S. Roundy, and P. K. Wright, "Anisotropic material properties of fused deposition modeling ABS," *Rapid Prototyp. J.*, vol. 8, no. 4, pp. 248–257, 2002.
3. Bellini, S. Güçeri, "Mechanical characterization of parts fabricated using fused deposition modeling," *Rapid Prototyp. J.*, vol. 9, no. 4, pp. 252–264, 2003.
4. D. P. B. S. J. Riddick, J.C. Hall, A.J. Haile, M.A. Wahlde, R.V. Cole, "Effect of Manufacturing Parameters on Failure in Acrylonitrile–Butadiane–Styrene Fabricated by Fused Deposition Modeling," *Struct. Dyn. Mater. Conf.*, vol. 53, no. April, pp. 1–8, 2012.
5. Durgun and R. Ertan, "Experimental investigation of FDM process for improvement of mechanical properties and production cost," *Rapid Prototyp. J.*, vol. 20, no. 3, pp. 228–235, 2014.
6. B. M. Tymrak, M. Kreiger, and J. M. Pearce, "Mechanical properties of components fabricated with open-source 3-D printers under realistic environmental conditions," *Mater. Des.*, vol. 58, pp. 242–246, 2014.
7. J. C. Riddick, M. A. Haile, R. Von Wahlde, D. P. Cole, O. Bamiduro, and T. E. Johnson, "Fractographic analysis of tensile failure of acrylonitrile-butadiene-styrene fabricated by fused deposition modeling," *Addit. Manuf.*, vol. 11, pp. 49–59, 2016.
8. C. Koch., L. Van Hulle, N. Rudolph, "Investigation of mechanical anisotropy of the fused filament fabrication process via customized tool path generation", Additive Manufacturing, 16, 2017, pp. 138-145.
9. Y. Zhang, Y.C. Yeoh, G. Zheng, S.K. Moon, "Characterization of mechanical properties of ULTEM 9085 using FDM", Proceedings of the International Conference on Progress in Additive Manufacturing, Singapore, 2018.
10. S.K. Selvamani, M. Samykano, S.R. Subramaniam, G. Kanagaraj, W.K. Ngui, Kadirgama, K., Idris, M.S., "3D printing: overview of ABS evolvement", AIP Conference Proceedings 2059, 2019.
11. A.R. Zekavat, A. Jansson, J. Larsson, L. Pejryd, "Investigating the effect of fabrication temperature on mechanical properties of fused deposition modeling parts using X-ray computed tomography" International Journal of Advanced Manufacturing Technology, 100, 2019, pp. 287-296.
12. B. Brenken, E. Barocio, A. Favaloro, V. Kunc, R.B. Pipes, Fused filament fabrication of fiber-reinforced polymers: A review, Additive Manufacturing, Volume 21, 2018, pp. 1-16
13. ASTM International, Designation: D2344/2344M-16, "Standard Test Method for Short-Beam Strength of Polymer Matrix Composite Materials," vol. i, pp. 1–8, 2018.

14. J. Comer *et al.*, "Mechanical characterisation of carbon fibre-PEEK manufactured by laser-assisted automated-tape-placement and autoclave," *Compos. Part A Appl. Sci. Manuf.*, vol. 69, pp. 10–20, 2015.

15. D. Zhang, D. Heider, and J. Gillespie, John W., "Void reduction of high-performance thermoplastic composites via oven vacuum bag processing," *J. Compos. Mater.*, 2017.

16. I. Fernandez, F. Blas, and A. Frovel, "Autoclave forming of thermoplastic composite parts," *J. Mater. Process. Technol.*, vol. 143, pp. 266–269, Dec. 2003.

17. Technical Data Sheet "FDM Nylon 12CF" from Stratasys

18. Toray Carbon Fibers America, "M55J DATA SHEET MJ type high modulus fiber with enhanced tensile and compressive strength over CARBON," pp. 6–7.

19. F. N. Cogswell, Thermoplastic aromatic polymer composites : a study of the structure, processing, and properties of carbon fibre reinforced polyetheretherketone and related materials. Oxford [England]; Boston: Butterworth-Heinemann, 1992.

20. C. M. Stokes-Griffin and P. Compston, "The effect of processing temperature and placement rate on the short beam strength of carbon fibre-PEEK manufactured using a laser tape placement process," *Compos. Part A Appl. Sci. Manuf.*, vol. 78, pp. 274–283, 2015.

21. C. E. Materials, "Technical Data Sheet - CYCOM 5276 Epoxy Resin System," *AECM - 00009*, pp. 1–7.

22. Symposium on Toughened Composites (1985 : Houston, *Toughened composites : Symposium on Toughened Composites*. Philadelphia, PA : American Society for Testing and Materials, 1987.

23. H. Saidpour and M. Barikani, "Mode-II Interlaminar Fracture Toughness of Carbon/Epoxy Laminates," *Iran. Polym. J.*, vol. 12, no. 5, pp. 389–400, 2003.

24. S. Gao and J. Kim, "Cooling rate influences in carbon fibre / PEEK composites . Part III : impact damage performance," *Compos. Manuf.*, vol. 32, pp. 775–785, 2001.

25. "A comprehensive review of the materials properties of VICTREX ® PEEK ™ high performance polymer," *www.victrex.com*. .

26. R. F. Gibson, "Principals of Composite Material Mechanics", CRC Press, 4th Ed., 2016

27. R. Jen, C.H. Lee, Strength and life in thermoplastic composite laminates under static and fatigue loads. Part II", , In. J. Fatigue, Vol 20, No. 9 pp 617-629, 1998

28. N. Rudolph, D. Zhang, P. Woytowitz, "Making the first 3D printed carbon fibre bike", JEC Composites Magazine, No. 125, Nov-Dec 2018.